

Critical behavior of the magnetic susceptibility of the uniaxial ferromagnet LiHoF_4

P. Beauvillain and J.-P. Renard

*Institut d'Electronique Fondamentale, Laboratoire associé au Centre National de la Recherche Scientifique
Bâtiment 220, Université Paris-Sud, 91405 Orsay Cédex, France*

I. Laursen

Department of Electrophysics, Building 322, The Technical University of Denmark, DK-2800, Lyngby, Denmark

P. J. Walker

Clarendon Laboratory, Parks Road, Oxford, United Kingdom

(Received 21 February 1978).

The magnetic susceptibility of two LiHoF_4 single crystals has been measured in the range 1.2–4.2 K. Ferromagnetic order occurs at $T_c = 1.527$ K. Above 2.5 K, the susceptibilities parallel and perpendicular to the fourfold c axis are well interpreted by the molecular-field approximation, taking into account the ground state and the first excited state of Ho^{3+} in the crystal field of S_4 symmetry. The experimental results are consistent with $g_{\parallel} = 13.95$ and $g_{\perp} = 0$ for the ground state. The dipolar contribution to the magnetic interaction is about three times larger than the exchange one. Near T_c , the parallel susceptibility is well described by the classical law with logarithmic corrections theoretically predicted by Larkin and Khmel'mitskii for the uniaxial dipolar ferromagnet or by a power law with a critical-exponent value $\gamma = 1.05$ rather close to 1. The upper limit of the critical region is $(T_{\text{max}} - T_c)/T_c = 1.1 \times 10^{-2}$.

I. INTRODUCTION

The compounds $\text{LiR}_x\text{Y}_{1-x}\text{F}_4$ where R is a rare earth, crystallized in the tetragonal scheelite structure $I4_1/a$.¹ They are efficient laser materials² and can be used for frequency conversion in the infrared-visible region.³ Due to their practical interest, many experimental studies have been done on these materials: chiefly, absorption and fluorescence⁴ and electron paramagnetic resonance (EPR).⁵⁻⁷

Another exciting characteristic of these compounds, especially those with 100% rare earth, is their low-temperature magnetic behavior. Indeed, one can expect that the rare-earth atoms which are fairly ionic are predominantly coupled by dipole-dipole interaction. Moreover, the high-point symmetry through the rare earth and the relative simplicity of the crystal structure allow theoretical calculations. Recently, Misra and Felsteiner⁸ have theoretically studied the magnetically ordered state of the LiRF_4 by a generalization of the Luttinger-Tisza method, considering only dipole-dipole interactions between rare-earth ions. They predicted ferromagnetism for $g_{\parallel} > g_{\perp}$ and antiferromagnetism for $g_{\parallel} < g_{\perp}$ where g_{\parallel} and g_{\perp} are, respectively, the Landé tensor component parallel and perpendicular to the c axis. At this time, the magnetic phase transition has been observed only for $R = \text{Tb}$, Ho , and Er . Both LiTbF_4 ($T_c = 2.874$ K)⁹ and LiHoF_4 ($T_c = 1.53$ K)^{10,11} are ferromagnets with the easy axis along c and LiErF_4 was

found to order antiferromagnetically¹² ($T_N = 0.381$ K) with the spins lying in the aa plane. This is consistent with the theoretical predictions since for LiErF_4 $g_{\perp} \gg g_{\parallel}$, while for LiTbF_4 and LiHoF_4 g_{\perp} is close to zero and g_{\parallel} is rather large, respectively, 17.85 and 14.1.⁶ Both LiTbF_4 and LiHoF_4 appear as nearly ideal uniaxial ferromagnets.

Critical phenomena in such uniaxial systems with dipolar interactions are extremely interesting. Indeed, in this special case the marginal dimensionality d^* above which the critical behavior is classical, i.e., given by the Landau theory, is $d^* = 3$ instead of $d^* = 4$ for systems with short-range interactions.¹³ At the marginal dimensionality, Larkin and Khmel'nitskii¹⁴ (LK) predicted logarithmic correction terms to the Landau-like critical behavior. This was further supported by Aharony¹⁵ and Brézin and Zinn-Justin¹⁶ for uniaxial dipolar ferromagnets.

In particular, the susceptibility should diverge as $t^{-1} |\ln t|^{1/3}$ rather than as the Landau form of t^{-1} , t being the reduced temperature $|T - T_c|/T_c$. One difficulty in observing logarithmic corrections to the mean-field power laws arises from the fact that these corrections are only valid in the limit of $T \rightarrow T_c$ whereas experiments are always carried out at a finite distance from T_c . Aharony and Halperin¹⁷ have suggested from their renormalization group (RG) analysis that the form $\ln(t/t_0)$ is used to analyze experimental data with t_0 being an adjustable parameter. Detailed comparisons between RG theory and experi-

ments on LiTbF_4 are now available. In the specific heat the logarithmic divergence is the leading singularity and high-precision experiments of Ahlers *et al.*¹⁸ were indeed consistent with a $|\ln(t/t_0)|^{1/3}$ behavior and with an amplitude ratio of $\frac{1}{4}$ for the specific heat above and below T_c as predicted. Aharony and Halperin¹⁷ pointed out that the RG equations implied an exact relationship between the spin correlation range and the specific-heat data. The neutron scattering data by Als-Nielsen¹⁹ confirmed this relation accurately. In addition he found that the amplitude ratio of the susceptibility above and below T_c had the mean-field and RG value of 2. Finally, very accurate spontaneous magnetization data were obtained by Griffin *et al.*²⁰ using Faraday rotation, and although the leading singularity here is a power law with exponent β , they concluded that $\beta = \frac{1}{2}$ with logarithmic corrections did fit the data better than the best-fit power law with $\beta = 0.38$.

The compounds LiRF_4 are fair but not ideal model systems of the uniaxial dipolar coupled ferromagnet. With $R = \text{Tb}$ the ground state is actually not an Ising doublet, but is split by a small amount due to the crystal field. Higher excited states are present albeit at energies considerably above $k_B T_c$, and finally exchange interactions are present in addition to the dipolar interaction. All these effects are different in LiHoF_4 , and we have therefore initiated a study of the critical behavior of this substance to supplement the information available from LiTbF_4 .

We report here measurements of parallel and perpendicular susceptibility of LiHoF_4 in order to define the Landé tensor components g_{\parallel} and g_{\perp} and the exchange and dipolar contributions to magnetic interaction between rare-earth ions. Since these measurements confirmed that LiHoF_4 is a rather good uniaxial dipolar ferromagnet, we performed very accurate parallel susceptibility measurements in the critical region and tried to discriminate between the theoretically predicted classical law with logarithmic corrections $t^{-1}|\log_{10}t|^{1/3}$ and the usual power law $t^{-\gamma}$.

II. EXPERIMENTAL TECHNIQUES

A. Crystal growth and sample preparation

The measurements were performed on two different LiHoF_4 samples. Sample 1 was grown at the Lyngby Technical University of Denmark by the method previously described by Laursen and Holmes.⁷ It was ground into an ellipsoid of $7.26 \times 1.92 \times 1.24 \text{ mm}^3$ with its long axis parallel to c , weighing $53.2 \pm 0.2 \text{ mg}$.

Sample 2 was grown by Walker at Oxford Clarendon Laboratory using also the Stockbarger method. A monocrystalline part of optical quality was selected and ground into a sphere of $4.836 \pm 0.002\text{-mm}$ diam

and $339.8 \pm 0.2\text{-mg}$ weight. In both cases, the starting materials were of purity $>99.9\%$ and the crystal quality was controlled by x-ray diffraction.

B. Susceptibility measurements and thermometry

Magnetic susceptibility was measured by means of an ac mutual inductance bridge²¹ operating at 70 Hz. The susceptibility probe was calibrated against chromium-potassium alum with a precision of about 1%. The amplitude of the ac measuring field was kept as low as 2 Oe in order to avoid nonlinear effects, especially close to T_c . The bridge balance was achieved by sample extraction. The sample and the probe were directly immersed in a pumped ^4He bath. Above 2.17 K, helium pressure was stabilized by a Cartesian manostat. Below 2.17 K, an electronic stabilization of the ^4He bath was achieved by a commercial temperature controller²² (ac resistance bridge ATNE). The temperature sensor was a $47\text{-}\Omega$, $\frac{1}{8}\text{-W}$ Allen Bradley carbon resistor. Temperature stability was better than 0.1 mK in this range. Temperature was obtained from a germanium resistor²³ thermally anchored to the sample and its Teflon holder by a bundle of 200 thin copper wires. It was measured with an ATNE ac resistance bridge and calibrated against the ^4He vapor pressure using T_{58} scale. The ^4He pressure was determined from an oil manometer and a commercial pressure gauge.²⁴ Above 2.17 K, ^4He is not superfluid and its pressure corresponds to the surface temperature which appreciably differs from that inside the bath. In this range the germanium resistor was calibrated against the magnetic susceptibility of CrK alum. The reproducibility and the precision of the thermometer are discussed in detail in Sec. III.

C. Sample orientation

Sample 1 (ellipsoid) was oriented by the conventional Laue-x-ray technique and set in a long cylindrical holder inside the susceptibility probe. The spherical sample 2 was set in a Teflon conical holder and its orientation was achieved *in situ* by applying a dc magnetic field. Since $g_{\parallel} \gg g_{\perp}$, fields of about 200 Oe were large enough to orientate the c axis along the field with a precision better than 1° at 4.2 K. Vertical and horizontal dc fields were, respectively, produced by a solenoid coaxial to the susceptibility probe and a pair of Helmholtz coils.

III. EXPERIMENTAL RESULTS AND DISCUSSION

A. Parallel and perpendicular susceptibilities in the range 1.2–4.2 K

The measured susceptibilities per gram χ_{\parallel}^m , and χ_{\perp}^m of sample 2, in the temperature range 1.2–4.2 K are

given in Fig. 1. χ_{\perp}^m is much smaller than χ_{\parallel}^m . This reflects the strong anisotropy of the g tensor in the ground state. χ_{\parallel}^m reaches a plateau below $T_c = 1.526 \pm 0.004$ K at a maximum value of $(4.195 \pm 0.040) \times 10^{-2}$ emu cgs which corresponds to $1/N\rho = 4.175 \times 10^{-2}$ emu cgs, where $N = \frac{4}{3}\pi$ is the sphere demagnetizing factor and $\rho = 5.72$ the crystal density. This variation of χ_{\parallel}^m versus temperature is consistent with a transition at T_c to a ferromagnetic state with the Ho^{3+} spins along the c crystal axis, in agreement with previous measurements by Cooke *et al.*¹¹ and Hansen *et al.*¹⁰

To explain the experimental data well above T_c (2.5–4.2 K), we used the Ho^{3+} energy scheme in LiHoF_4 proposed by Hansen *et al.*¹⁰ and Margariño and Tuchendler.²⁵ In a crystal field of S_4 symmetry, the $(2J+1)$ -fold degenerate ground term 5I_8 is split into a fundamental doublet $\Gamma_{3,4}$ and a first excited Γ_2 singlet of energy $E_1/k_B = 10.4 \pm 0.4$ K. The other excited states are well above and they only give the temperature-independent Van Vleck contributions to low-temperature susceptibility. A straightforward calculation leads to the following expression for the parallel susceptibility χ_{\parallel}^m of the isolated Ho^{3+} ion (neglecting the interactions):

$$\chi_{\parallel}^m = \frac{n\mu_B^2}{4k} \frac{(g_{\parallel}^0)^2 T^{-1} + a_{\parallel}^0 + a_{\parallel}^1 e^{-E_1/kT}}{1 + 0.5e^{-E_1/kT}}, \quad (1)$$

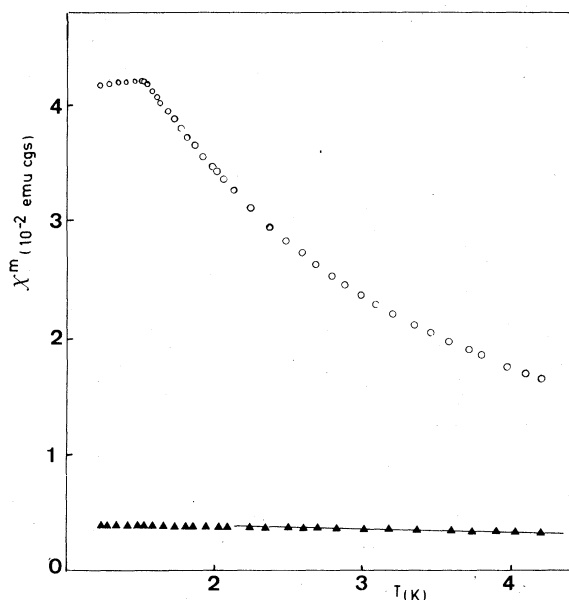


FIG. 1. Experimental parallel susceptibility per gram χ_{\parallel}^m (open circles) and perpendicular susceptibility per gram χ_{\perp}^m (black triangles) vs temperature for the spherical sample. The solid line represents the approximate theoretical law, for $e^{-E_1/kT} \ll 1$: $\chi_{\perp}^m = (n\mu_B^2/4k)(B + Ce^{-E_1/kT})$, with $B = 9.98$, $C = 11.3$, and $E_1/k = 10.4$ K.

where n is the number of Ho atoms per gram, μ_B the Bohr magneton, k the Boltzman constant, g_{\parallel}^0 the Landé tensor component along c for the ground state, and a_{\parallel}^0 , a_{\parallel}^1 the respective Van Vleck contributions of the ground state and of the first excited state. When we take into account the interaction between Ho^{3+} ions in a simple mean-field approximation, we obtain for χ_{\parallel}^m

$$\chi_{\parallel}^m = \chi_{\parallel}^m / (1 - \alpha_{\parallel} \chi_{\parallel}^m), \quad (2)$$

where the parameter α_{\parallel} contains the dipolar and exchange contributions to the interaction (see Fig. 2).

The best fit of relations (1) and (2) to the experimental data between 2.5 K and 4.2 K is achieved for $g_{\parallel}^0 = 13.95 \pm 0.15$, $a_{\parallel}^0 = 0.25 \pm 0.1$, $a_{\parallel}^1 \approx 3.3 \pm 1.5$, and $\alpha_{\parallel} = -1.6 \pm 0.4$ (emu cgs)⁻¹. The g_{\parallel}^0 value is in good agreement with the EPR one⁶ $g_{\parallel}^0 = 14.1 \pm 0.2$ but it differs significantly from that of Ho^{3+} diluted in LiYF_4 : $g_{\parallel}^0 = 13.3 \pm 0.1$. It also slightly differs from the value of 13.6 ± 0.2 determined from previous susceptibility measurements.¹¹ However, these measure-

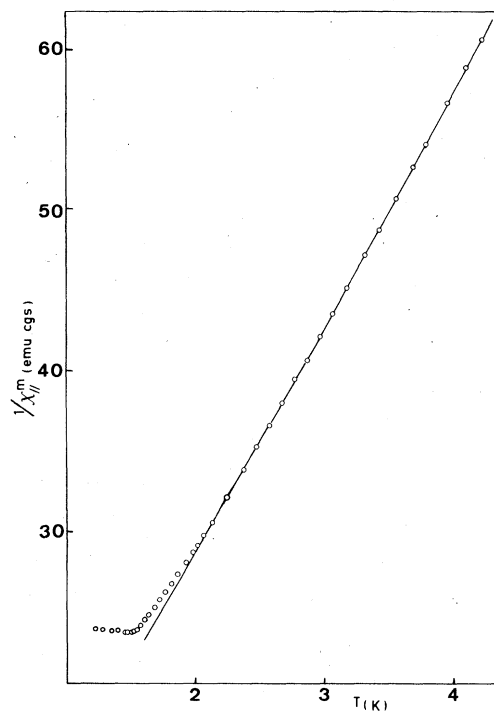


FIG. 2. Reciprocal experimental parallel susceptibility per gram $1/\chi_{\parallel}^m$ vs temperature for a spherical sample. The solid line represents the theoretical curve $1/\chi_{\parallel}^m = 1/\chi_{\parallel}^m - \alpha_{\parallel}$ with

$$\chi_{\parallel}^m = \frac{n\mu_B^2}{4k} \left[\frac{(g_{\parallel}^0)^2 T^{-1} + a_{\parallel}^0 + a_{\parallel}^1 e^{-E_1/kT}}{1 + 0.5e^{-E_1/kT}} \right]$$

with $\alpha_{\parallel} = -1.6$, $g_{\parallel}^0 = 13.95$, $a_{\parallel}^0 = 0.25$, $a_{\parallel}^1 = 3.3$, and $E_1/k = 10.4$ K.

ments were interpreted by the simple Curie-Weiss law: $\chi_{\parallel}^m = C_m/T - \Theta$. Fitting our experimental data with this Curie-Weiss law in the range 2.5–4.0 K leads to $g_{\parallel} = 13.55 \pm 0.1$, $C_m = (6.95 \pm 0.1) \times 10^{-2}$ emu cgs and $\Theta = +0.02 \pm 0.04$ K in good agreement with Ref. 11. Our value of a_{\parallel}^1 is rather imprecise and will be improved by further χ_{\parallel} measurements above 4.2 K.

The α_{\parallel} value can be easily related to dipolar and exchange interactions. The local field \bar{H}_{loc} at a rare-earth-ion site is given by

$$\bar{H}_{\text{loc}} = [1 + (\frac{4}{3}\pi\rho - \bar{\delta} + \bar{\epsilon} - \bar{N}\rho) \cdot \bar{\chi}] \cdot \bar{H} \quad (3)$$

where \bar{H} is the external field, $\bar{\chi}$ the susceptibility tensor, and $\bar{\delta}$, $\bar{\epsilon}$, and \bar{N} are, respectively, the dipolar, exchange, and demagnetizing field tensor. $\bar{\delta}$ is expressed as follows:

$$\bar{\delta} = n^{-1} \sum_i \frac{\bar{r}_i^2 - 3\bar{r}_i\bar{r}_i}{r_i^5} \quad (4)$$

where \bar{r}_i is the vector to the i th rare-earth neighbor.

Due to the S_4 symmetry, all tensors are diagonal in a coordinate system which contains the fourfold axis c . For a spherical sample $\bar{N} = \frac{4}{3}\pi\bar{I}$ and α_{\parallel} is simply given by

$$\alpha_{\parallel} = \epsilon_{\parallel} - \delta_{\parallel} \quad (5)$$

where ϵ_{\parallel} and δ_{\parallel} denote the tensor components along c .

δ_{\parallel} has been calculated from (4) by summing over the Ho^{3+} sites inside a sphere of 400-Å diam. Taking into account the obtained value of $\delta_{\parallel} = -9.5$ and the experimental α_{\parallel} , we determined $\epsilon_{\parallel} = -11.1 \pm 0.4$. This exchange contribution is much smaller than the total dipolar one: $\frac{4}{3}\pi\rho - \delta_{\parallel} = 33.46$. The corresponding exchange energy in the ground state $zJ/4k = n\epsilon_{\parallel}(g_{\parallel}^0\mu_B)^2/4k = -0.820 \pm 0.03$ K may be compared to that of LiErF_4 : $zJ/4k = -0.620$ K. We can also describe the mass perpendicular susceptibility χ_{\perp}^m using formulas (1) and (2) with the character \perp instead of \parallel . Since $g_{\perp} = 0$ and $\exp(-E_1/kT) \ll 1$, χ_{\perp}^m takes the approximate form

$$\chi_{\perp}^m = \frac{n\mu_B^2}{4k} (B + Ce^{-E_1/kT})$$

with

$$B = a_{\perp}^0(1 + \alpha_{\perp}Aa_{\perp}^0) \quad \text{and} \quad C = a_{\perp}^1 + a_{\perp}^0(\alpha_{\perp}Aa_{\perp}^1 - 0.5)$$

with $A = n\mu_B^2/4k$.

The best fit in the range 2.8–4.2 K is obtained for $B = 9.98 \pm 0.05$ and $C = 11.3 \pm 0.7$. The present temperature range is too restricted to obtain independently a_{\perp}^0 , a_{\perp}^1 , and α_{\perp} .

B. Critical behavior of the parallel susceptibility

We have measured accurately the parallel susceptibility of LiHoF_4 in the range 1.5–1.8 K. Two and four successive experimental runs were done, respectively, on samples 1 and 2. Temperature of the sample and thermometer was kept below 77 K between runs in order to avoid calibration drift and nonreproducibility of the thermometer. Each run contained about 60 points. Helium vapor pressure was carefully measured at about 20 points for calibrating the germanium resistor thermometer. In the considered temperature range, the experimental values $T(R)$ are accurately fitted by the empirical Clement and Quinell relation (Fig. 3):

$$T^{-1} = a \log_{10}R + b(\log_{10}R)^{-1} + c \quad (6)$$

The parameters a, b, c were obtained by the least-squares method. For each selected calibration point, the difference between temperatures obtained from the T_{58} scale and from relation (6) is less than 0.3 mK.

The measured parallel susceptibility χ_{\parallel}^m of sample 2 in the temperature range 1.52–1.65 K is shown on Fig. 4. Owing to the resolution of the ac mutual inductance bridge of 4×10^{-7} emu cgs, the data of the four different experimental runs are very well consistent with each other.

We have compared the experimental χ_{\parallel}^m data for both samples 1 and 2 to the classical law with logarithmic corrections theoretically predicted by LK¹⁴:

$$\chi_c = At^{-1}|\log_{10}t|^{1/3} \quad (7)$$

and to the power law

$$\chi_c = A't^{-\gamma} \quad (8)$$

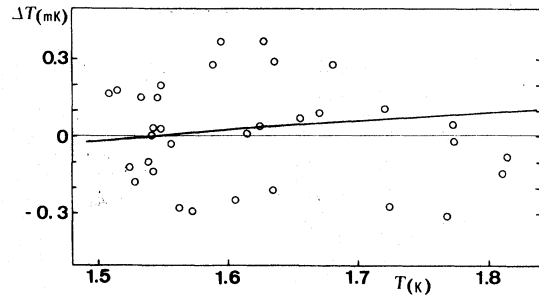


FIG. 3. Plot of ΔT , the difference between temperatures obtained from the T_{58} scale and from the empirical Clement and Quinell relation (1) $T^{-1} = a \log_{10}R + b(\log_{10}R)^{-1} + c$ with $a = 0.749801$, $b = 7.578944$, and $c = -4.439235$ vs temperature in the range 1.5–1.8 K. The solid line represents the difference between temperatures obtained with relation (1) for two different sets of parameters: the a , b , and c values reported above and $a' = 0.750987$, $b' = 7.599984$, $c' = -4.449258$ corresponding to least-squares fit for, respectively, four and three different runs.

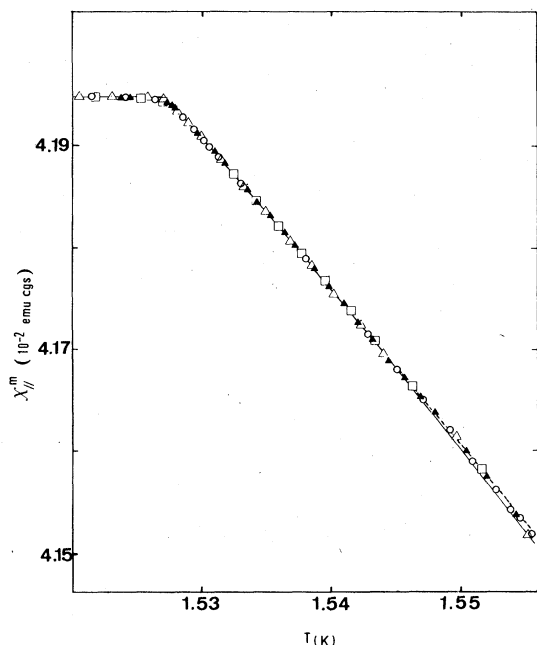


FIG. 4. Experimental parallel susceptibility per gram vs temperature in the range 1.52–1.56 K for four different runs on the spherical sample. Full line represents the classical law with logarithmic corrects and dashed line the power law with parameter values of Table I.

where t is the reduced temperature $t = (T - T_c)/T_c$ and χ_c the susceptibility corrected from the demagnetizing field effect. χ_{\max} being the maximum value of $\chi_{||}^m$, we define $\chi_{\text{th}}(t)$ by

$$[\chi_{\text{th}} t]^{-1} = \chi_c^{-1}(t) + \chi_{\max}^{-1} \quad (9)$$

In the case of the theoretical LK law (7), we have to adjust three parameters: χ_{\max} , T_c , and A for the best fit of χ_{th} to the experimental data. We also introduce two additional parameters T_{\min} and T_{\max} which are the limits of the temperature range of the fit. One of these parameters χ_{\max} is relatively well defined from the susceptibility measurements just below T_c . Thus for a given value of χ_{\max} , and for a series of T_c values, we determine the A values which give the best fit to the experimental data in the range $T_{\min} < T < T_{\max}$.

In Fig. 5, we have plotted the average difference

$$\Delta = \frac{1}{N} \sum_i |\chi_{\text{th}}(t_i) - \chi_{||}^m(t_i)|$$

where N is the number of experimental points between T_{\min} and T_{\max} versus A . For a given T_c , A is determined as the value which corresponds to the minimum of $\Delta(A)$. The best T_c value corresponds to the $\Delta(A)$ curve which has the lower minimum. For various intervals $T_{\min} - T_{\max}$, the best T_c and A values are obtained by this procedure. We observed that these T_c and A values do not depend on the interval $T_{\min} - T_{\max}$ provided that T_{\min} is outside the

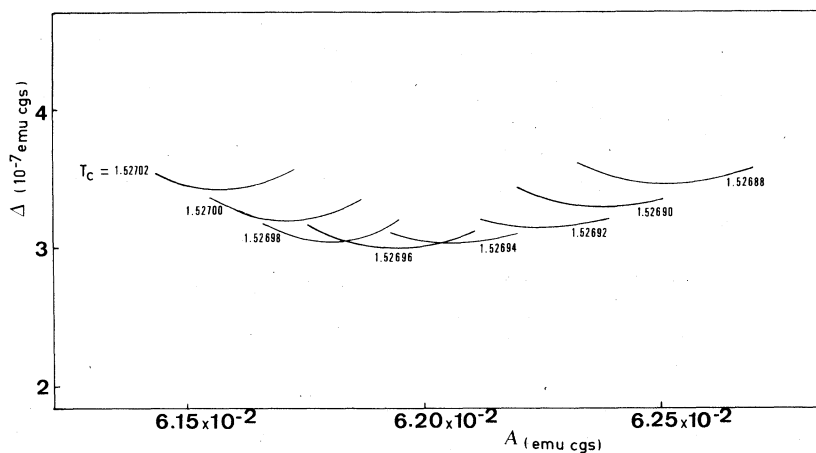


FIG. 5. Average difference Δ vs critical amplitude A for different values of T_c and for a given value of $\chi_{\max} = 4.1952 \times 10^{-2}$ emu cgs and $T_{\max} = 1.544$ K, $T_{\min} = 1.5273$ K.

$$\Delta = (1/N) \sum_i |\chi_{\text{th}}(t_i) - \chi_{||}^m(t_i)|$$

where N is the number of experimental points in the range $T_{\min} < T < T_{\max}$. $\chi_{||}^m$ is the parallel susceptibility per gram of the spherical sample and χ_{th} is the theoretical susceptibility for a critical behavior with logarithmic corrections:

$$1/\chi_{\text{th}}(t) = 1/At^{-1} |\log_{10} t|^{1/3} + 1/\chi_{\max}$$

The best fit is obtained for $T_c = 1.52696$ and $A = 6.195 \times 10^{-2}$.

TABLE I. Critical temperature and amplitude for the magnetic mass susceptibility of LiHoF_4 for the classical law with logarithmic correction $\chi_c^m = A t^{-1} |\log_{10} t|^{1/3}$ and the power law $\chi_c^m = A' t^{-\gamma}$; χ_c^m is the mass susceptibility corrected for demagnetizing field effect, χ_{\max} is the maximum value of the measured mass susceptibility along the easy axis, t is the reduced temperature $(T - T_c)/T_c$, and $\Delta = (1/N) \sum_i |\chi_{\text{th}}(t_i) - \chi_{\text{m}}^m(t_i)|$ is the average difference between the theoretical susceptibility and the measured susceptibility on the N experimental points in the temperature range $1.5273 < T < 1.544$ K.

		χ_{\max}	T_c	A	Δ	
Classical law with logarithmic corrections	Sample 1	0.21957	1.52560	6.356×10^{-2}	3.7×10^{-7}	
	Sample 2	4.1952×10^{-2}	1.52696	6.195×10^{-2}	3.0×10^{-7}	
		χ_{\max}	T_c	A'	γ	Δ
Power law	Sample 1	0.21957	1.52567	6.364×10^{-2}	1.05	2.1×10^{-7}
	Sample 2	4.1952×10^{-2}	1.52700	6.216×10^{-2}	1.05	2.9×10^{-7}

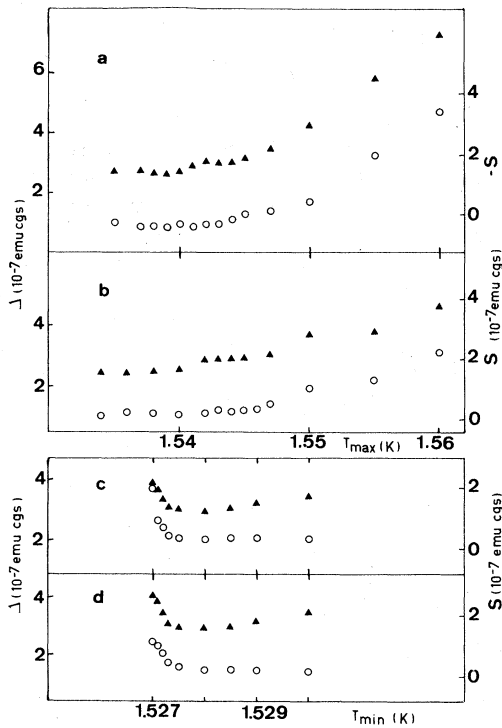


FIG. 6. Δ (black triangle) and S (white circle) vs T_{\max} and T_{\min} . Δ is the average difference $(1/N) \sum_i |\chi_{\text{th}}(t_i) - \chi_{\text{m}}^m(t_i)|$ and S the algebraic sum $\sum_i [\chi_{\text{th}}(t_i) - \chi_{\text{m}}^m(t_i)]$ on the N experimental points in the temperature range $T_{\min} < T < T_{\max}$. For a critical behavior with the values of critical parameters indicated in Table I for sample 2, we have plotted the following for a classical law with logarithmic corrections: (a) Δ and $-S$ vs T_{\max} with $T_{\min} = 1.5273$ K; (c) Δ and S vs T_{\min} with $T_{\max} = 1.544$ K; for a power law: (b) Δ and S vs T_{\max} with $T_{\min} = 1.5273$ K; (d) Δ and S vs T_{\min} with $T_{\max} = 1.544$ K.

rounding near T_c and t_{\max} does not exceed 10^{-2} . The final values of the parameters which give the best fit to experimental data are reported in Table I for both samples 1 and 2. The experimental data of the parallel susceptibility of sample 2 and the difference with the theoretical laws (7) and (8) versus temperature are given in Table II.

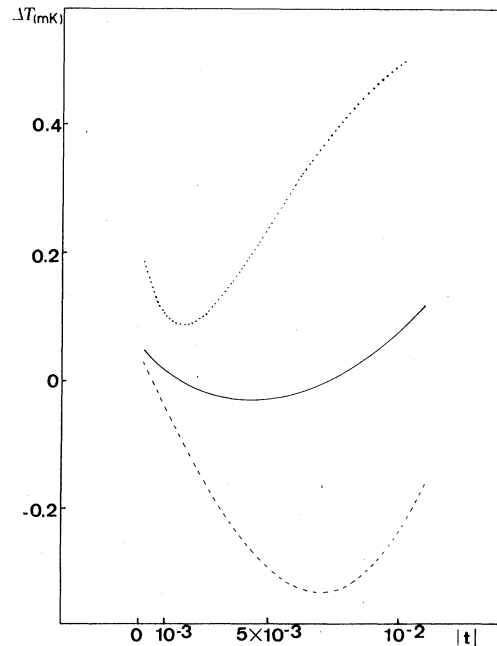


FIG. 7. $\Delta T = T_c(t' - t)$ vs t where t is the reduced temperature $(T - T_c)/T_c$. We have plotted (full line) ΔT for our critical susceptibility measurements on LiHoF_4 assuming $A t^{-1} |\log_{10} t|^{1/3} = A' t^{-\gamma}$. We have also plotted vs t using the temperature difference between the power law and the classical law with logarithmic corrections for the specific-heat measurements of Ahlers *et al.* (Ref. 18) on LiTbF_4 ; dashed line for $T > T_c$ and dotted line for $T < T_c$.

TABLE II. Experimental parallel susceptibility $\chi_{||}$ of sample 2 of LiHoF_4 (spheroid sample of 4.836 ± 0.002 -mm diam and 339.8 ± 0.2 -mg weight) versus temperature. We have also reported the difference versus temperature between the experimental data and the two theoretical laws:

$\Delta\chi_{\text{in}} = At^{-1}|\log_{10}t|^{1/3} - \chi_{||}$; $\Delta\chi_{\text{pow}} = A't^{-\gamma} - \chi_{||}$; with the values of the parameters indicated in Table I.

T	χ (10^{-2} emu cgs)	$\Delta\chi_{\text{in}}$ (10^{-6} emu cgs)	$\Delta\chi_{\text{pow}}$ (10^{-6} emu cgs)
1.5434	1.41739	-11.1	-5.8
1.5415	1.41841	-12.6	-9.6
1.5396	1.41938	-8.6	-7.7
1.5377	1.42030	-1.5	-1.9
1.5359	1.42120	1.3	0
1.53413	1.42289	9.8	8.3
1.52895	1.42464	-0.4	-0.2
1.52707	1.42535	13.0	14.0
1.52529	1.42545	7.0	7.0
1.52438	1.42550	2.0	2.0
1.52356	1.42552	0.0	0.0
1.5218	1.42552	0.0	0.0
1.54325	1.41741	-5.1	0
1.5421	1.41801	-3.9	-0.2
1.5410	1.41854	1.1	3.4
1.53983	1.41918	-1.3	-0.2
1.53868	1.41978	-1.3	-0.9
1.53726	1.42051	-0.2	-0.9
1.53640	1.42096	-0.8	-1.9
1.53528	1.42154	-1.3	-2.8
1.53433	1.42199	1.7	0.4
1.53348	1.42242	1.7	0.2
1.53251	1.42295	-3.2	-4.7
1.53176	1.42331	-2.6	-4.1
1.53101	1.42370	-4.5	-5.6
1.53013	1.42404	3.6	3.0
1.52959	1.42428	5.8	5.6
1.52897	1.42460	2.8	3.0
1.52867	1.42477	-0.4	0.1
1.52825	1.42500	-4.7	-3.9
1.52788	1.42513	-3.0	-1.7
1.52762	1.42520	4.3	5.6
1.52722	1.42535	6.0	8.0
1.52687	1.42539	13.0	13.0
1.52600	1.42545	7.0	7.0
1.52540	1.42545	7.0	7.0
1.52360	1.42550	2.0	2.0
1.5421	1.41796	4.7	4.1
1.5420	1.41888	9.0	10.5
1.5385	1.41983	3.9	4.1
1.53685	1.42064	8.1	7.3
1.5350	1.42164	2.1	0.9
1.5332	1.42890	9.4	7.9
1.5316	1.42338	-1.3	-2.4
1.5299	1.42419	-0.4	-2.6
1.5290	1.42462	-0.6	-0.2
1.5281	1.42505	-2.1	-1.1
1.52765	1.42520	3.0	4.3

TABLE II. (Continued)

T	χ (10^{-2} emu cgs)	$\Delta\chi_{\text{in}}$ (10^{-6} emu cgs)	$\Delta\chi_{\text{pow}}$ (10^{-6} emu cgs)
1.52737	1.42526	8.8	10.3
1.52782	1.42518	-2.4	-1.3
1.52721	1.42530	12.0	13.0
1.52688	1.42541	11.0	11.0
1.52601	1.42548	4.0	4.0
1.52501	1.42550	2.0	2.0
1.52482	1.42550	2.0	2.0
1.52303	1.42552	0.0	0.0
1.51967	1.42554	-2.0	-2.0
1.5428	1.41758	1.7	6.2
1.53304	1.42261	4.5	3.0
1.53247	1.42293	8.3	-0.6
1.53127	1.42349	4.1	3.0
1.53063	1.42383	1.1	0.2
1.53014	1.42406	1.1	0.4
1.52939	1.42443	0.2	0.2
1.52903	1.42460	0.	0.2
1.52861	1.42481	-1.9	-1.3
1.52822	1.42496	0.9	1.7
1.52790	1.42513	-1.7	-0.6
1.52768	1.42518	3.9	5.1
1.52746	1.42528	3.0	5.0
1.52726	1.42533	7.0	8.0
1.52710	1.42535	11.0	13.0
1.52695	1.42537	15.0	15.0
1.52671	1.42539	13.0	13.0
1.52607	1.42541	11.0	11.0
1.52426	1.42548	4.0	4.0
1.52151	1.42552	0.0	0.0

With the parameters of Table I for sample 2 we obtain in the temperature range $1.5273 < T < 1.544$

$$s^2 = \frac{1}{N-F} \sum_i [\chi_{\text{th}}(t_i) - \chi_{\text{fl}}(t_i)]^2$$

$$= 2.15 \times 10^{-13} \text{ emu cgs} ,$$

where F is the number of fit parameters and $\chi^2 = 1.34$.

A similar fit procedure has been adopted with the power law.⁸ In this case there is an additional parameter γ , and $\Delta(A')$ curves were systematically drawn for different values of T_c and γ . The resulting best values of these parameters are given in Table I and we obtain for sample 2: $s^2 = 1.91 \times 10^{-13}$ emu cgs and $\chi^2 = 1.19$.

A slight change of χ_{max} does not appreciably affect the amplitudes A and A' and the exponent γ but shifts T_c of the same quantity for both laws (7) and (8). The observed small discrepancies between the samples 1 and 2 are probably due to their completely different origin and especially to different impurity contents.

We have also studied the influence of T_{min} and T_{max} on the average difference

$$\Delta = \frac{1}{N} \sum_i |\chi_{\text{th}}(t_i) - \chi_{\text{fl}}^m(T_i)|$$

and on the algebraic sum

$$S = \sum_i [\chi_{\text{th}}(t_i) - \chi_{\text{fl}}^m(t_i)] ,$$

all other parameters being fixed at their values in Table I. Figure 6(a) shows Δ and $-S$ vs T_{max} . They remain small until $T_{\text{max}} \approx 1.544$ and strongly increase when temperature exceeds this value. The same phenomenon is observed for both laws (7) and (8). This $T_{\text{max}} \approx 1.544$ K which corresponds to a relative temperature $t_{\text{max}} \approx 1.1 \times 10^{-2}$ can be considered as the upper limit of the critical region. This extension of the critical region is consistent with the values reported for LiTbF_4 ($t_{\text{max}} \sim 10^{-2}$),¹⁸ and GdCl_3 ($t_{\text{max}} = 1.15 \times 10^{-2}$).²⁶ In Fig. 6(c), we have plotted Δ and S vs T_{min} for a fixed T_{max} value of 1.544 K. In

sample 2, the rounding effect starts at $T_{\min} = 1.5273$ K which corresponds to $t_{\min} \approx 2 \times 10^{-4}$. It appears that the rounding effect is smaller in this LiHoF_4 samples than that observed on LiTbF_4 ($t_{\min} = 10^{-3}$) and GdCl_3 ($t_{\min} = 1.5 \times 10^{-3}$).

Finally, we are not able to discriminate between the laws (7) and (8) on the basis of the present experimental data. The average difference of the best fit to the data is, respectively, equal to 3.0×10^{-7} and 2.9×10^{-7} emu cgs for the laws (7) and (8) on sample 2. Assuming $A t^{-1} |\log_{10} t|^{1/3} = A' t'^{-\gamma}$, we have calculated the temperature difference $\Delta T = T_c(t' - t)$ vs T (Fig. 7). The maximum ΔT value is equal to 0.1 mK in the critical temperature range. Since the T_{58} temperature scale has absolute errors of about 2 mK and an internal point to point roughness of 0.1 mK,²⁷ it would be rather difficult to improve the thermometry

in the actual temperature range and to bring forward discrimination between the considered critical laws.

IV. CONCLUSION

The present susceptibility measurements confirm that LiHoF_4 is a fairly good uniaxial dipolar ferromagnet. The parallel susceptibility is accurately fitted by the classical law with logarithmic corrections predicted by Larkin and Khmel'nitskii. Nevertheless we could not discriminate between this theoretical law and a power law with a critical exponent rather close to 1. This discrimination would require an improved temperature scale with a point to point roughness better than 0.01 mK at 1.5–1.6 K. Magnetization and specific-heat measurements in the critical region would be useful to complete this study. Further work is in progress.

-
- ¹R. E. Thoma, G. D. Brunton, R. A. Penneman, and T. K. Keenan, *Inorg. Chem.* **9**, 1096 (1970).
²E. P. Chicklis and C. S. Naiman, *IEEE J. Quantum Electron.* **QE 8**, 535 (1972).
³R. K. Watts and W. C. Holton, *Solid State Commun.* **9**, 137 (1971).
⁴H. P. Jenssen, A. Linz, R. P. Leavitt, C. A. Morrison, and D. E. Westman, *Phys. Rev. B* **11**, 92 (1975); J. E. Miller and E. J. Sharp, *J. Appl. Phys.* **41**, 4718 (1970); A. L. Harmer, A. Linz, and D. R. Gabbe, *J. Phys. Chem. Solids* **30**, 1483 (1969); M. R. Brown, K. G. Rooth, and W. A. Shand, *J. Phys. C* **2**, 593 (1969).
⁵J. P. Sattle and J. Nemanich, *Phys. Rev. B* **4**, 1 (1971); J. Margariño, J. Tuchendler, J. P. D'Haenens, and A. Linz, *Phys. Rev. B* **13**, 2805 (1976).
⁶J. Margariño and J. Tuchendler, *Physica* **86-88B**, 1233 (1977).
⁷I. Laursen and L. M. Holmes, *J. Phys. C* **7**, 3765 (1974).
⁸S. K. Misra and J. Felsteiner, *Phys. Rev. B* **15**, 4309 (1977).
⁹L. M. Holmes, T. Johansson, and H. J. Guggenheim, *Solid State Commun.* **12**, 993 (1973).
¹⁰P. E. Hansen, T. Johansson, and R. Nevald, *Phys. Rev. B* **12**, 5315 (1975).
¹¹A. H. Cooke, D. A. Jones, J. F. A. Silva, and M. R. Wells, *J. Phys. C* **8**, 4083 (1975).
¹²P. Beauvillain, J.-P. Renard, and P. E. Hansen, *J. Phys. C* **10**, L709 (1977).
¹³See, for instance, K. G. Wilson and J. Kogut, *Phys. Rev. C* **12**, 75 (1974).
¹⁴I. A. Larkin and D. E. Khmel'nitskii, *Zh. Eksp. Teor. Fiz.* **65**, 2087 (1969) [*Sov. Phys.-JETP* **29**, 1123 (1969)].
¹⁵A. Aharony, *Phys. Rev. B* **8**, 3363 (1973).
¹⁶E. Brézin and J. Zinn-Justin, *Phys. Rev. B* **13**, 251 (1976).
¹⁷A. Aharony and B. I. Halperin, *Phys. Rev. Lett.* **35**, 1308 (1975).
¹⁸G. Ahlers, A. Kornblit, and H. J. Guggenheim, *Phys. Rev. Lett.* **34**, 1227 (1975).
¹⁹J. Als-Nielsen, *Phys. Rev. Lett.* **37**, 1161 (1976).
²⁰J. A. Griffin, J. D. Litster, and A. Linz, *Phys. Rev. Lett.* **38**, 251 (1977).
²¹B. Lécuyer, Thèse CNAM (Paris, 1969) (unpublished).
²²ATNE, Z. A. Courtaboeuf, 91400 Orsay, France.
²³Ge resistor model N2, Scientific Instruments, Lake Worth, Texas.
²⁴Pressure gauge, Texas Instruments, Dallas Road, Bedford, Texas.
²⁵J. Margariño and J. Tuchendler (unpublished).
²⁶J. Kötzler and G. Eiselt, *Phys. Lett. A* **58**, 69 (1976).
²⁷J. R. Clement, *Temperature*, (Reinhold, New York, 1962), Vol. 3, p. 67.